Scientific
Research

Morphology and Optical Measurements of Nanostructured In₂O₃:SnO₂ Nanoparticle

A. Ayeshamariam[1*], M. Jayachandran[2], C. Sanjeeviraja[3], M. Tajun Meera Begam[4]

[1]Department of Physics, Khadir Mohideen College, Adirampattinam, India
[2]ECMS Division, CECRI, Karaikudi, India
[3]School of Physics, Alagappa University, Karaikudi, India
[4]Department of Chemistry, Avvaiyar Government College for Women, Karaikal, India
Email: [*]ashamma786@yahoo.com

ABSTRACT

Ultra-fine and uniform ITO nanopowders can be prepared by very simple Combustion method. In this paper, effects of Indium oxide with Sn doping on crystallinity, band gap values by UV studies and morphological studies by SEM and TEM analysis of nanopowders are reported. Powder mixtures of In₂O₃:SnO₂ of 90:10 compositions are prepared and calculated grain size from X-ray diffraction measurements. The free electron absorption is determined from spectral transmission and reflection measurements. Key words: In₂O₃:SnO₂, XRD, UV, Combustion and SEM.

Keywords: In₂O₃:SnO₂; XRD; UV; Combustion; SEM

1. Introduction

In₂O₃:SnO₂ (also called indium tin oxide or ITO) is a highly degenerate n-type wide gap semiconductor that is produced by doping Sn atoms in In₂O₃. Since ITO powders have a high transmittance in the visible range and a high conductivity simultaneously, they are widely used in a variety of electronic and optoelectronic fields. In Combustion process In₂O₃:SnO₂ powders show an interesting and technologically important combination of properties: they have luminous transmittance, high infrared reflectance, good electrical conductivity, excellent substrate adherence, hardness, and chemical inertness. Composite powders have been patented for use as agrochemicals and herbicides. Parent *et al*. [1] used extended X-ray absorption fine structure (EXAFS) investigations and found that the In atomic environment was modified by the Sn doping. Even at low tin concentrations the first oxygen polyhedron and the metallic In-In co-ordination shells were disordered. This disorder increases with the amount of tin inserted. Tin doped indium oxide is extensively studied as a base material for its gas sensor applications. It is oxygen deficient and therefore is an n type semiconductor with a wide band gap (3.53 eV) [2]. The effect of crystallite size on the optical properties has been widely studied [3]. Nanocrystalline powders have attracted considerable interest because of their high transmittance. Here, we have presented the optical properties

of 90:10 nanocrystalline ITO powders [4].

1.1. Physical Characterization

The visible transmission was recorded using Hitachi S3400N Spectrophotometer. The calcined powders were further characterized by particle size analysis (Autosizer IIC Malvern) and powder X-ray diffraction (XRD) (X-ray diffractometer (XRD) with monochromation CuK$_\alpha$ target (1.5406 Å) at a scan rate of 2°C/min). Unit cell parameter was calculated from the observed "d"-spacing, which was accurately measured with the help of silicon as an internal standard. Particle size and morphology of the synthesized powders were further evaluated with the help of a transmission electron microscope TEM (JEOL JEM 200CX). Scanning electron microscope (SEM) and Energy dispersive X-ray analysis (EDAX) work on the calcined powders were performed under Scanning Electron Microscope Cambridge 53400N and elemental analysis was studied by EDAX Make "thermo software Norton systems". The asprepared powders were pelletised at a pressure of 500 kg/m².

1.2. Experimental

The Combustion method is a useful technique that has been shown to be good preparation route for ITO nanopowders [5]. It is based on exothermic and usually very rapid chemical reaction between metal nitrates as an oxidizer and an organic fuel [6], such as Urea, glycine and so on.

---

[*]Corresponding author.

A key feature of the method is that heat is required to maintain the chemical reaction supplied from the reaction itself that is not from an external source but from an internal one. Therefore to achieve an optimized combustion reaction condition, many chemical reaction parameters must be considered [7]. Among known fuels we used the urea which had the versatility of combustion synthesis methods by showing successful preparation of a large number of well crystallized multicomponent oxides [8]. The raw materials used in this study are $In(NO_3)_2 \cdot 2H_2O$, $Sn(NO_3)_2 \cdot 3H_2O$, these raw materials were dissolved in distilled water and mixed in a appropriate ratio to form a tin nitrate solution. Then urea $(CO(NH_2)_2)$ was added to this solution. The amount of urea was fixed at 1.0 mol [9]. Amount of urea was calculated based on total valence of the oxidizing and reducing agents for maximum release of energy during combustion. Oxidant/fuel ratio of the system was adjusted by adding nitric acid and ammonium hydroxide; and the ratio was kept at unity. The solution was heated under constant stirring at a temperature of about 60°C in a Pyrex vessel on a hot plate. Then the concentration of the solution slowly became higher. The resulting translucent solution was heated on a hot plate (at about 100°C) until it turned into a viscous solution. The solution boils upon heating and undergoes dehydration accompanied by foam. The foam then ignites by itself due to persistent heating giving a voluminous and fluffy product of combustion. The combustion product was subsequently characterized as single phase nanocrystals of ITO. The resulting ashes were then fired at a temperature higher than 350°C until complete decomposition of the residues was achieved. Yellow ashes obtained after combustion were then collected for structural characterization and other morphological studies. The system was homogeneous during the whole process and no precipitation was observed. The entire processing steps are illustrated in **Figure 1**. The final mixtures are heated for two different temperatures of 300°C and 500°C.

2. Results and Discussion

2.1. XRD

Structural studies by XRD showed the presence of dominant β-phase with a minor quantity of α-phase. The atomic arrangements in the grain boundary seem to be somewhat different from regular periodic arrangement whereas inside the grain there is a good periodic arrangement of atoms. **Figure 2(a)** shows the XRD structure of different temperature. XRD lines are indicating that Sn has gone to the substitutional position forming solid solution. XRD shows complete oxidation of the alloy giving mainly cubic phase of In_2O_3. The crystallite size of the nanocrystalline powder is estimated using Scherer formula [10]. Average value of grain size varies from 9 nm to 18
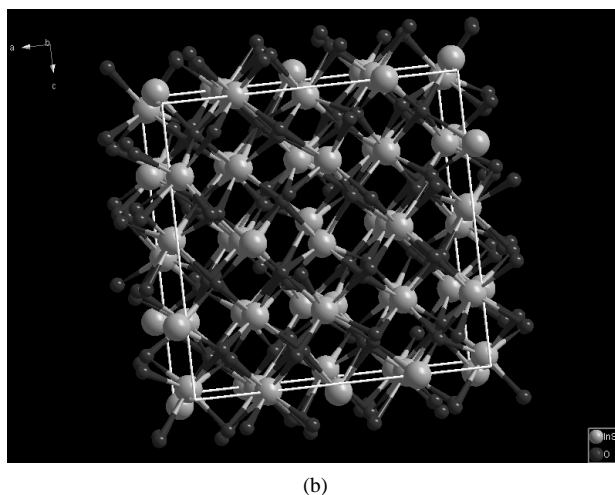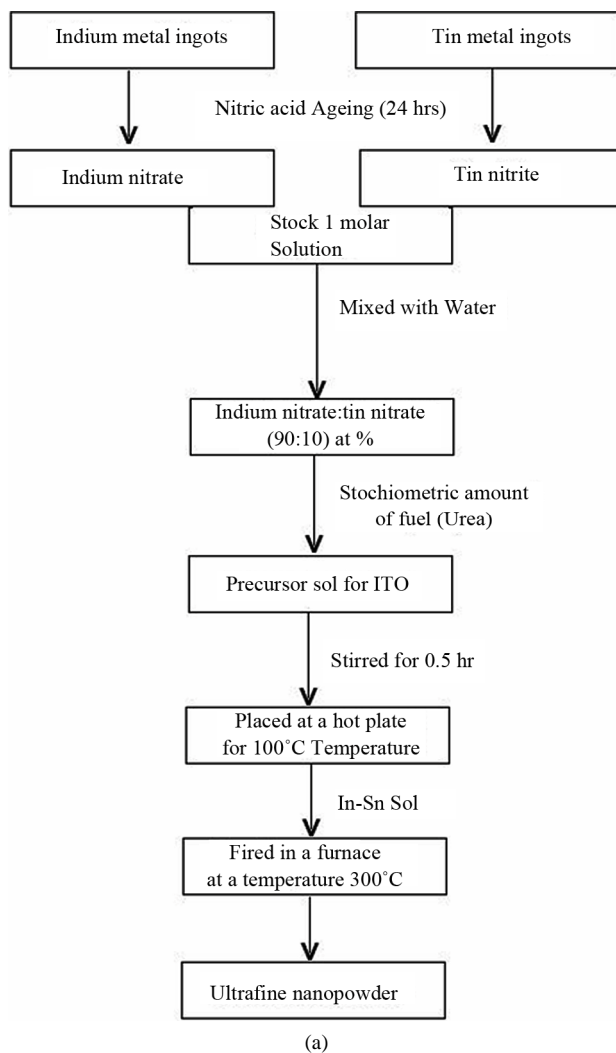

(a)

(b)

Figure 1. (a) Schematic representation of precursor sol preparation and ultra fine powder by Combustion synthesis; (b) XRD of proportions (90:10).

nm for the prominent of peak (222) (400), (440) and (622) orientation. From the figures the analysis of crystal struc-

ture revealed that the detected peak of the nanoparticle was corresponded with that of crystallized ITO. That is very intense peak was found at the three most important peaks of In_2O_3 namely (222), (400) and (440) reflections. The diffraction patterns are well matched with TEM results shown in **Figure 3**. EDAX analysis confirmed the prepared nanoparticles were fine indium tin oxide powdered and there was no impurity in it as shown in **Figure 5**.

ITO materials retain the cubic structure upto the solubility limit of the SnO_2 in In_2O_3 [11] at 90:10 doping concentrations when the temperature increases the lattice constant also increases rapidly. Then the tin ions occupy In_1 and In_2 sites shown in **Figure 1(b)**. The stoichiometric balance can be maintained only if additional oxygen is inserted into the lattice. These oxygen atoms can fill the empty tetracheal sites in the bixbyite structure. They tend mainly to gather near the Sn ion on In_2 sites and can form strongly bound O-Sn-O units. This occupation mechanism does not produce additional free electrons. The increase in conductivity is only small. Larger doping concentrations cause a further oxygen reception. Apart from the $O-Sn_2-O$ units $O-Sn_1-O$ arrangements can also occur. This effects a further distortion of the bix-byte structure. The microstrain increases and the domain size decreases which is shown in **Figures 2(b)-(d)**. The grain size strain values are shown in **Table 1**.

2.2. UV Studies

It was reported that, the model developed by Franck and Kostlin [12] for *tin* insertion into In_2O_3 results from an analysis of the carrier concentration and additional measurements of the lattice constants dependent on the doping
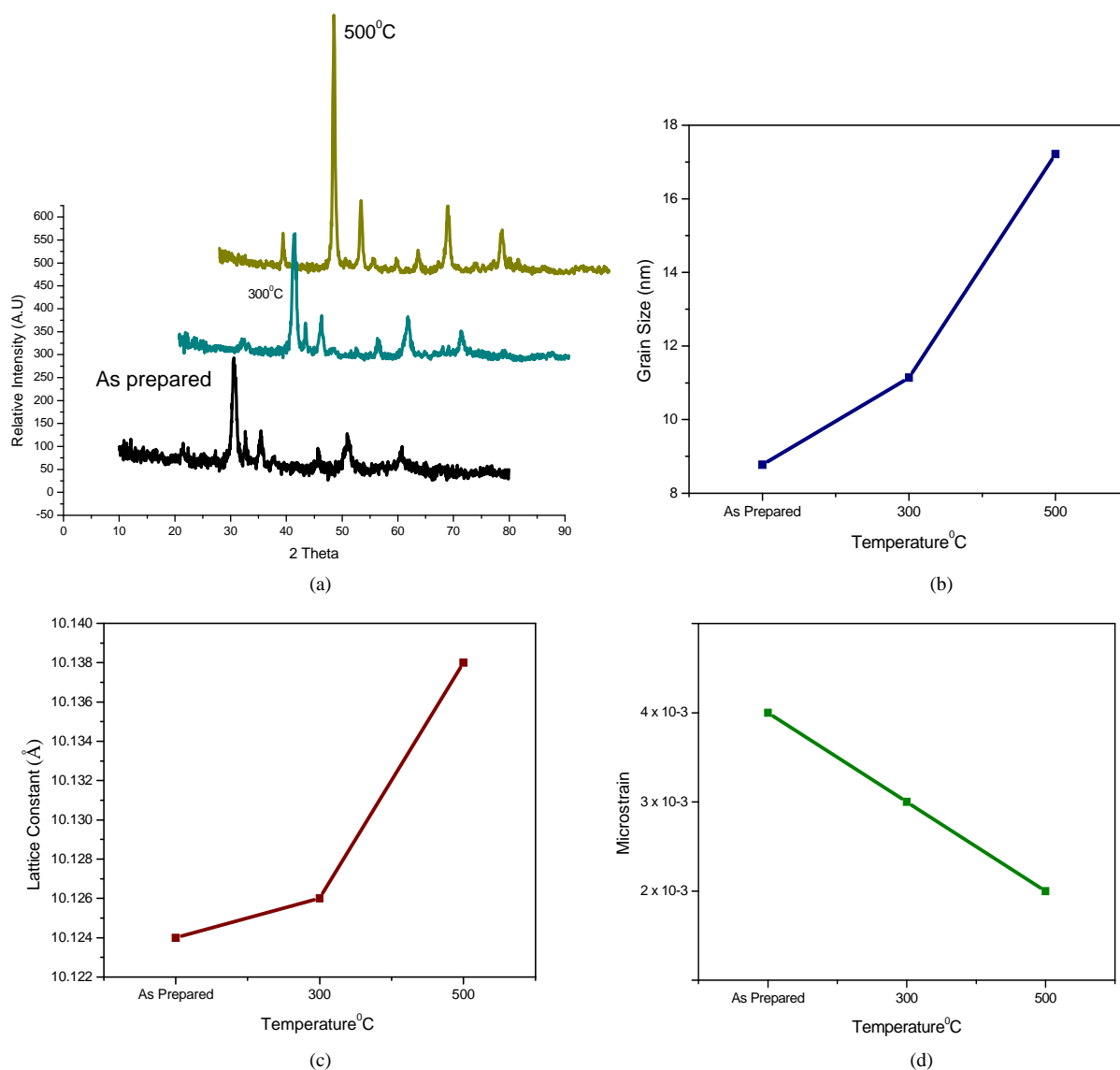

Figure 2. (a) XRD analysis for two different temperatures; (b) Grain Size; (c) Lattice Constant; (d) Micro strain.
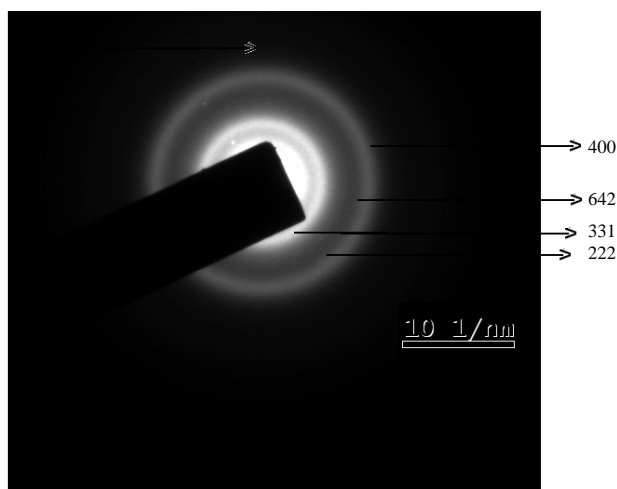

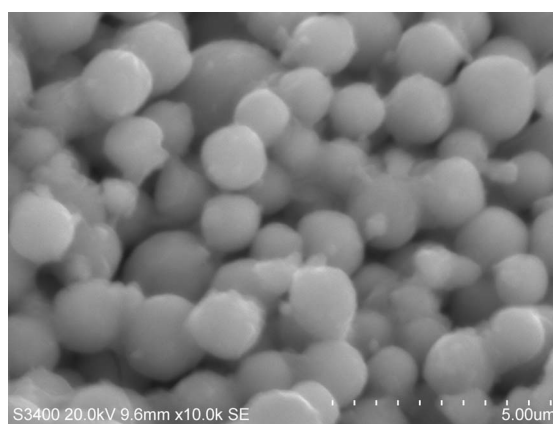**Figure 3. SAED for as prepared sample.**

Table 1. XRD results of ITO.

Sample (ITO)	Grain Size (nm)	Lattice Constant (Å)	Micro strain lines/m^2
As Prepared	8.776	10.124	4×10^{-3}
300°C	11.142	10.126	3×10^{-3}
500°C	17.217	10.138	2×10^{-3}

concentration. Optical analysis comprises two kinds of interstitial oxygen, one of which is loosely bound to *tin*, while the other forms a strongly bound Sn_2O_4 complex. At low doping concentration (10% Sn) here we found decreasing lattice constants and therefore concluded a dominance of the loosely bound *tin-oxygen* defects. Optical absorbance and transmission (T) spectra **Figures 6(a)-(c)** were measured using a near-infrared to UV double-beam spectrometer. Optical absorption coefficients (α) were calculated by correcting the reflection using a formula $\alpha = k\left(h\gamma - E_g\right)^{n/2} / h\gamma$, where E_g is the optical band gap (Tauc gap) and n is a constant. Using the model with $n = 2$ proposed by Tauc, E_g was estimated by linearly extrapolating the plot of $\sqrt{\alpha h v}$ vs $h v$ and finding the intersection with the abscissa (Tauc Plot) [13,14] shown in **Figures 7(a)-(c)** and **8**. The band gap for different temperatures are shown in **Table 2**.
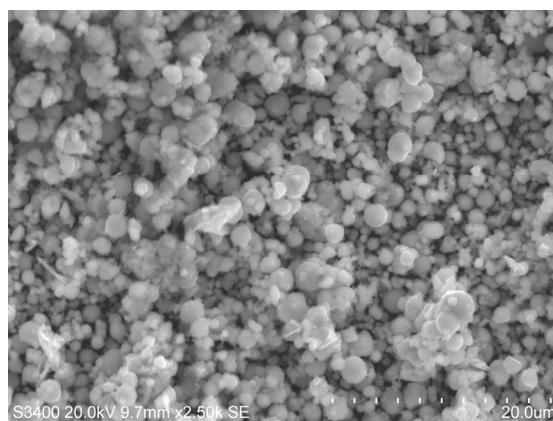
2.3. SEM Analysis

SEM photograph ITO (90:10) leading to an interconnected spherical structure with good mechanical strength. The nano-structural changes taking place during combustion process leads to a decrease in pore size and pore diameter. The nano-structural changes are accompanied by the associated internal stresses in the membrane. Increasing the annealing temperature with respect time can lead to local shifts in the interconnected grains, so as to reduce the internal stresses. It is well documented that the surface

morphology has a significant impact on the performance of nanostructure materials. The reaction temperature is one among them. We obtained surface spherical morphologies of ITO asprepared, 300°C and 500°C using ITO powder as source material. **Figures 4(a)-(c)** show Scanning Electron Microscopy (SEM) images of spherical-shaped ITO nano-structures at (100°C, 300°C and 500°C) different temperatures [15].

(a)

(b)
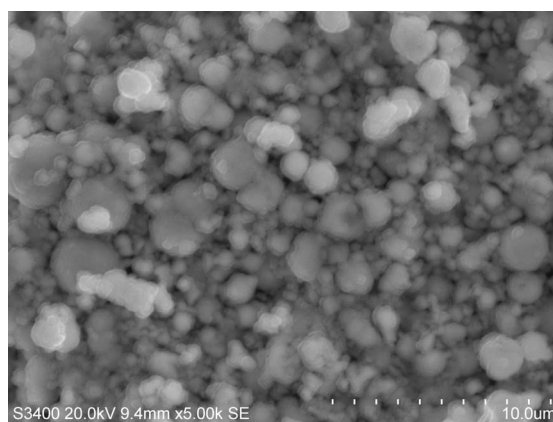
(c)

Figure 4. (a) SEM for asprepared sample; (b) SEM analysis at 300°C; (c) SEM analysis at 500°C.
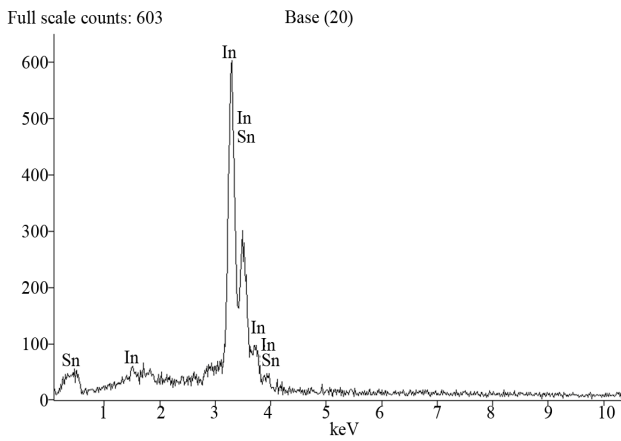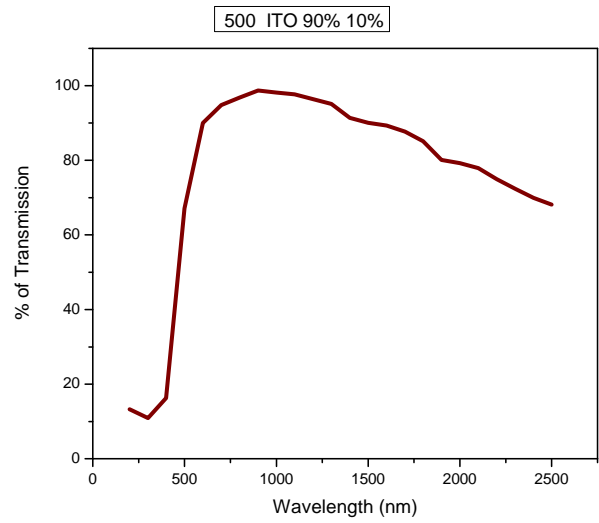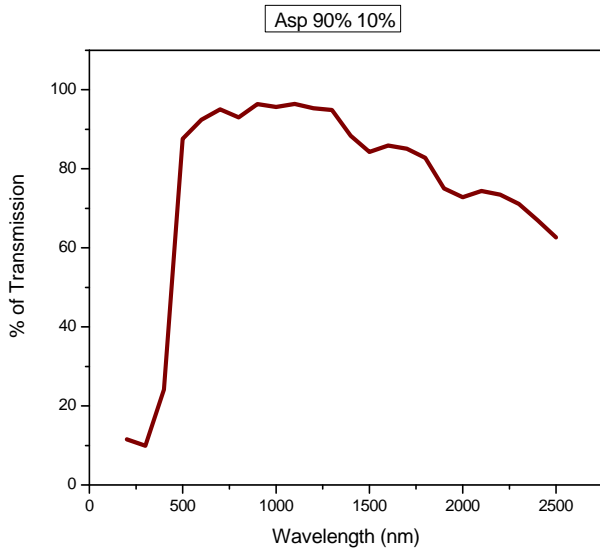
Full scale counts: 603   Base (20)
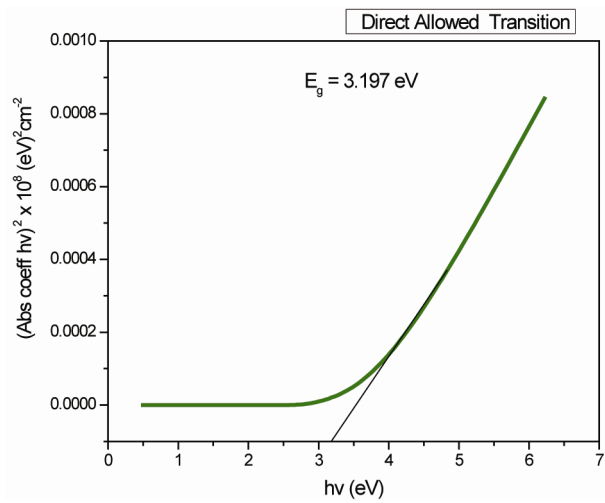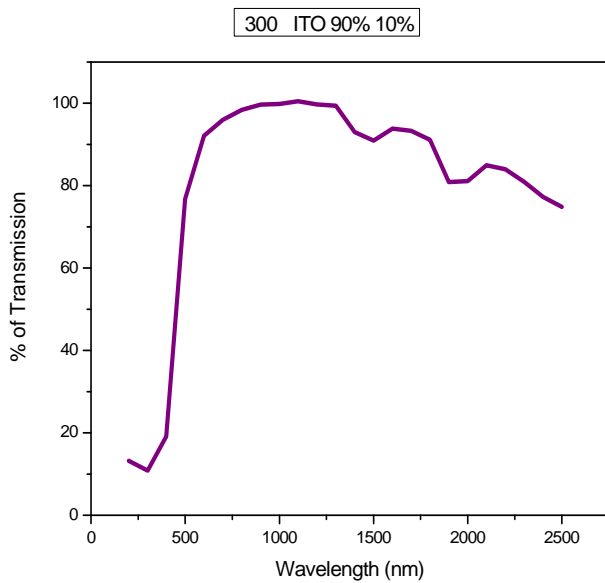

Figure 5. EDAX.

(c)

Figure 6. Transmittance curves of (a) ASP; (b) 300˚C; (c) 500˚C.
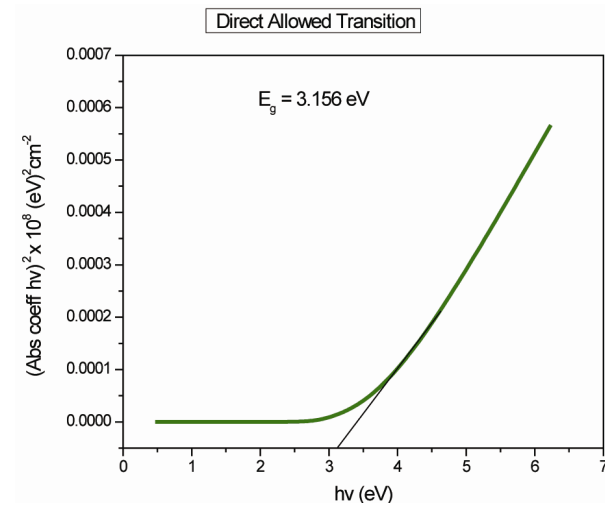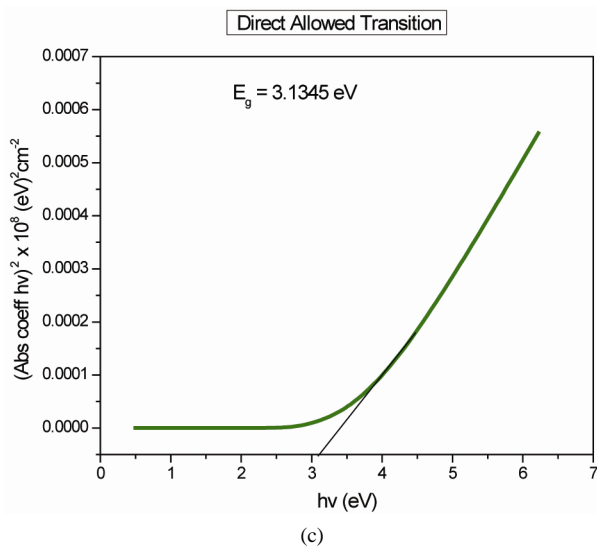

(a)

(b)

(a)

(b)

(c)

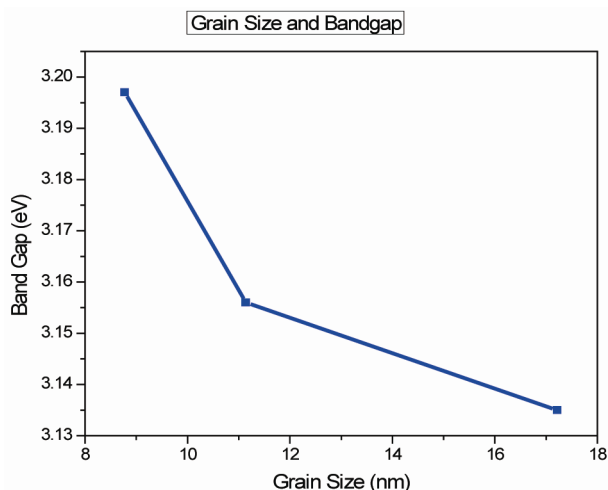**Figure 7. Band gap values of (a) ASP; (b) 300˙C; (c) 500˙C.**

Figure 8. Grain size and bandgap values of ITO.

Table 2. Bandgap values of ITO.

Sample (ITO)	Bandgap (eV)
As prepared	3.197
300˙C	3.156
500˙C	3.135

2.4. Sensor Analysis

The addition of a small amount of doping elements to SnO_2 powders has been known to be effective in modifying their optical and electrical properties [16]. In particular, in the case of gas sensor applications, a general strategy for tailoring materials for the selective sensor response involves the modification of the surface by the addition of dopants during sensor fabrication [17]. Hence, there is a growing interest in doping SnO_2 with different
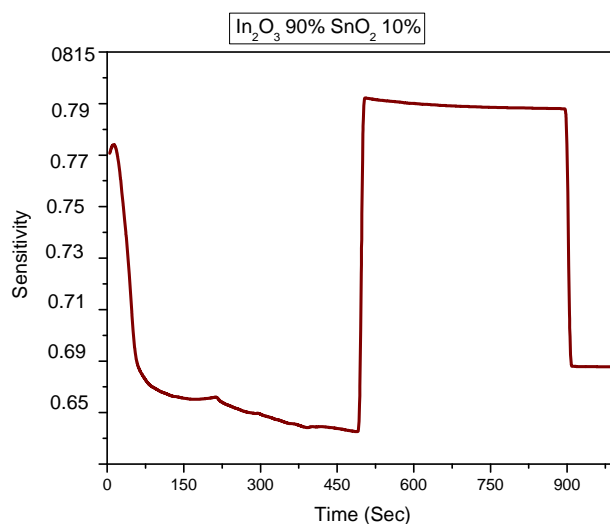

Figure 9. Sensitivity with respect to time of as prepared sample.

elements. In the present study, we observed increase in grain size due to increase in temperature. The grain size of the samples prepared is of the order of 9 nm. In this works, grain size effects on the sensitivity of gas sensor devices have been reported shown in **Figure 9**.

3. Conclusion

The experimental studies revealed that the sensitivity is enhanced when the grain size is decreased. Also Xu *et al.* [18] have observed that, by reducing the particle size (~6 nm), high gas sensitivity and short response times can be achieved. In our research the study of indium-doped SnO_2 powders, it has been concluded that uniform, homogenous and highly transparent powders with small grain size 9 nm can be prepared by indium doping on tin oxide. But the powders are highly resistive. Hence, In_2O_3:SnO_2 dopings can be used in areas where only a moderate electronic conductivity is required.

REFERENCES

[1] G. Franck and H. Kostlin, "Electrical Properties and Defect Model of Tin-Doped Indium Oxide Layers," *Applied Physics A*: *Materials Science & Processing*, Vol. 27, No. 4, 1982, pp. 197-206. doi:10.1007/BF00619080

[2] C. G. Fonstad and R. H. Rediker, "Electrical Properties of High-Quality Stannic Oxide Crystals," *Journal of Applied Physics*, Vol. 42, No. 7, 1971, p. 2911. doi:10.1063/1.1660648

[3] X. Wang, S. S. Yee and W. P. Carey, "Transition between Neck-Controlled and Grain-Boundary-Controlled Sensitivity of Metal-Oxide Gas Sensors," *Sensors and Actuators B*: *Chemical*, Vol. 25, No. 1-3, 1995, pp. 454-457. doi:10.1016/0925-4005(94)01395-0

[4] L. Abello, B. Bochu, A. Gaskov, S. Koudryavtseva, G.

Lucazeau and M. Roumyantseva, "Structural Characterization of Nanocrystalline SnO_2 by X-Ray and Raman Spectroscopy," *Journal of Solid State Chemistry*, Vol. 135, No. 1, 1998, pp. 78-85. doi:10.1006/jssc.1997.7596

[5]   J. H. Kang, J. Y. Kim and D. Y. Jeona, "Synthesis and Characterization of Orange Emitting SnO_2: Eu^{3+} Phosphor by an Optimized Combustion Method," *Journal of the Electrochemical Society*, Vol. 152, No. 3, pp. H33-H38.

[6]   L. E. Shea, J. Mukittrick and O. A. Lopez "Synthesis of Red-Emitting, Small Particle Size Luminescent Oxides Using an Optimized Combustion Process," *Journal of the American Ceramic Society*, Vol. 79, No. 12, 1996, pp. 3257-3265. doi:10.1111/j.1151-2916.1996.tb08103.x

[7]   S. R. Jain, K. C. Adiga and V. R. P. Verneker, "A New Approach to Thermochemical Calculations of Condensed Fuel-Oxidizer Mixtures," *Combustion and Flame*, Vol. 40, 1981, pp. 71-79. doi:10.1016/0010-2180(81)90111-5

[8]   A. S. Mukasyan, C. Costllo, K. P. Sherlock, D. Lafarga and A. Varma, "Perovskite Membranes by Aqueous Combustion Synthesis: Synthesis and Properties," *Separation and Purification Technology*, Vol. 25, No. 1-3, 2001, pp. 117-126. doi:10.1016/S1383-5866(01)00096-X

[9]   J. H. Kang, J. Y. Kim and D. Y. Jean, *Proceeding of the 3rd International Meeting on information display*, Daegu, 2002.

[10] H. Wulff and C. Eggs, "Investigation of Stored Energy in Plasma Deposited TiN_x Films," *Journal of Vacuum Science & Technology A*, Vol. 15, No. 6, 1997, p. 2938. doi:10.1116/1.580888

[11] A. R. Stokes, "A Numerical Fourier-Analysis Method for the Correction of Widths and Shapes of Lines on X-ray Powder Photographs," *Proceedings of the Physical Society*, Vol. 6, No. 4, 1948, p. 382. doi:10.1088/0959-5309/61/4/311

[12] Y. Ohhata, F. Shinoki and S. Yoshida, "Optical Properties of r.f. Reactive Sputtered Tin-Doped In_2O_3 Films," *Thin Solid Films*, Vol. 59, No. 2, 1979, pp. 255-261. doi:10.1016/0040-6090(79)90298-0

[13] J. Tauc, R. Grigorovici and A. Vancu, "Optical Properties and Electronic Structure of Amorphous Germanium," *Physica Status Solidi* (*b*), Vol. 15, No. 2, 1966, pp. 627-637. doi:10.1002/pssb.19660150224

[14] J. Tauc, "Amorphous and Liquid Semiconductors," In: J. Tauc, Ed., Plenum, New York, 1979.

[15] A. Gurlo, N. Barsan, U. Weimar, M. Ivanovskaya, A. Taurino and P. Siciliano, "Polycrystalline Well-Shaped Blocks of Indium Oxide Obtained by the Sol-Gel Method and Their Gas-Sensing Properties," *Chemistry of Materials*, Vol. 15, No. 23, 2003, pp. 4377-4383. doi:10.1021/cm031114n

[16] P. S. Devi, M. Chatterjee and D. Ganguli, "Indium Tin Oxide Nano-Particles through an Emulsion Technique," *Material Letters*, Vol. 55, No. 4, 2002, pp. 205-210. doi:10.1016/S0167-577X(01)00647-4

[17] S. Ramanan, "Dip coated ITO Thin-Films through Sol-Gel Process Using Metal Salts," *Thin Solid Films*, Vol. 389, No. 1-2, 2001, pp. 207-212. doi:10.1016/S0040-6090(01)00825-2

[18] H. Y. Xu, X. L. Liu, D. L. Cui, M. Li and M. H. Jiang, "A Novel Method for Improving the Performance of ZnO Gas Sensors," *Sensors and Actuators B*: *Chemical*, Vol. 114, No. 1, 2006, pp. 301-307. doi:10.1016/j.snb.2005.05.020